

Chapter 9

Other Applications



The CESE method has been applied to a wide range of scientific and engineering problems since its inception in the 1990s. Although solving CFD problem is the primary goal of the CESE method, this general approach is actually applicable to a variety of PDE systems with physical backgrounds different from fluid dynamics. This chapter mainly introduces the application highlights of CESE in several representative fields.

9.1 Hypersonic Aerodynamics

Typical high-speed aerodynamic problems can be solved by using the CESE methods. Successful examples of such applications include the supersonic flow over a blunted flat plate [1], Mach reflection of shock waves [2], unsteady viscous flows in rocket nozzles [3], counterflow jets for the reduction of aerothermal load on spacecrafts [4, 5], and the flow over roughness elements in a supersonic boundary layer [6].

With the increasing number of Mars exploration missions in recent years, the research interest of hypersonic aerothermodynamics has been revived. In a typical atmospheric-entry flight, the aircraft will encounter hypersonic gas flow, and the flow field is characterized by strong shock waves and thermochemical non-equilibrium effects. CFD has become a useful tool for in-depth understanding of complex flow physics and for complementary experimental prediction of aerodynamic characteristics.

Using a 2D axisymmetric CESE solver based on hybrid meshes, Wen et al. [7–9] conducted a systematic study of hypersonic chemically reacting non-equilibrium flows over spheres. Three different working gases: nitrogen, air, and carbon dioxide were used in their simulations. The thermochemical non-equilibrium effects considered therein include the vibrational energy relaxation of gas molecules as well as the dissociation and recombination reactions in the gas flows. The physically consistent coupled vibration–chemistry–vibration (CVCV) [10] two-temperature model was

employed. Here, the performance of the CESE method are shown by three different flow cases. The working gas, sphere radius, and the CESE simulation results [9] of the dimensionless shock stand-off distances (defined as the ratio of the stand-off distance to the sphere radius) of each case are listed in Table 9.1, along with the experimental and theoretical results of Wen and Hornung [11]. The CESE results are shown in good agreement with experimental and theoretical results. Further investigation of the shape of shock waves is presented in Fig. 9.1, in which the numerical density contours are overlaid on the experimental finite fringe differential interferograms. The shapes of the simulated bow shocks with the CESE method match the experimental results well.

Another important thermochemical non-equilibrium process in an atmospheric-entry flow is the ionization in a high-temperature shock layer. Massimi et al. [12] conducted a numerical investigation of hypersonic ionized air flows over rounded nose geometries, using a 2D axisymmetric CESE solver based on hybrid meshes. The multi-species NS equations were solved with the two-temperature seven-species Park model for ionization reactions. The weakly ionized air flow in the Radio Attenuation Measurement (RAM-C II) flight test at 71 km altitude was simulated and compared with experiments and numerical results of Candler and MacCormack [13]. The CESE results [12] of the maximum electron number densities along the direction normal to the vehicle's surface agree well with the flight test measurements and the numerical results of Candler and MacCormack [13].

Table 9.1 The working gases, sphere radii, and dimensionless shock stand-off distances (last three columns) in different flow cases

Case no	Gas	Radius (inch)	Experiment [11]	Theory [11]	Simulation [9]
1	N ₂	1.5	0.100	0.095	0.100
2	Air	1.0	0.105	0.093	0.095
3	CO ₂	2.0	0.088	0.084	0.087

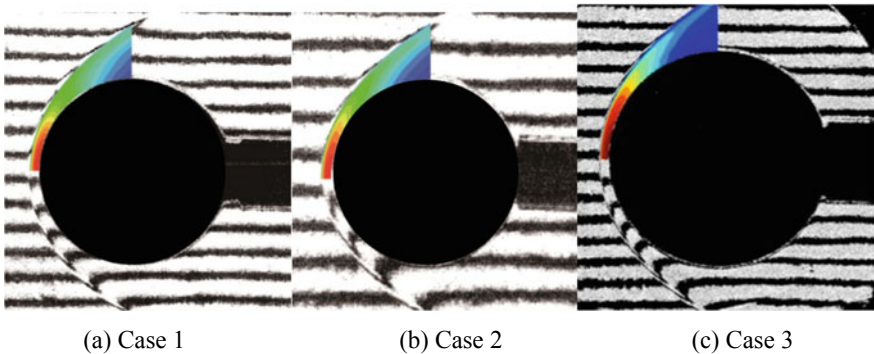


Fig. 9.1 Comparison of experimental shapes of the bow shocks with the numerical predictions by CESE. Courtesy of C. Y. Wen [9]

9.2 Aeroacoustics

Thanks to the rapid development of CFD, it is now expected to solve aeroacoustics problems through high-resolution numerical simulations of unsteady compressible Euler or NS equations. However, in many computational aeroacoustic problems, the coexistence of shock waves and small disturbances (acoustic waves) imposes stringent requirements on numerical methods.

The sound–shock interaction problem was used by Wang et al. [14] to examine the accuracy of the CESE method for aeroacoustic problems involving shock waves. Loh et al. [15] further considered three selected problems, namely a linear benchmark problem, instability waves on a free shear layer, and shock–vortex interactions, to illustrate the feasibility of using CESE as a tool for computational aeroacoustics (CAA). Good numerical results with high resolution and low dispersion were demonstrated by their second-order CESE scheme. Additionally, the authors also pointed out that the non-reflecting boundary condition, which plays an important role in CAA, is much simpler to implement in the CESE method than in traditional methods (see [15, 16]). To deal with practical multi-dimensional CAA problems where large disparity in grid cell size is inevitable, Yen et al. [17, 18] modified the Courant number insensitive (CNI)-CESE scheme [17] and the local time-stepping CESE scheme [18] to improve the numerical efficiency. A 3D simulation was performed for the propagation of a Gaussian acoustic pulse and a vorticity wave embedded in a Mach 0.5 mean flow. Once again, the CESE results were in good agreement with the corresponding analytical solution in preserving both the form and amplitude of the waves [17]. Yen [18] further conducted a series of 3D CESE simulations for the Helmholtz resonator problem. By using a second-order CESE scheme, excellent agreement between the linear acoustic theory and the CESE solution was achieved.

The CESE method has also been employed as a numerical tool for CAA problems in practical engineering applications related to engines and aircrafts. To shed light upon an aeroacoustic resonance phenomenon often encountered by convergent–divergent nozzles under transonic conditions, Loh and Zaman [19, 20] developed an axisymmetric NS solver using the CESE method and conducted a numerical investigation. A 3D CESE NS solver was also implemented by Loh et al. [15] and applied to compute the screech noise generated by an under-expanded supersonic jet. Kim et al. [21] simulated the supersonic unsteady flow over an open cavity to investigate the mixing-enhancement and flame-holding capability in the scramjet engine. The CESE method solving 2D NS equations successfully captured the self-sustained oscillations in the supersonic cavity flows. The computed frequencies and amplitudes of the pressure oscillations compare favourably with the theoretical and experimental data. Cheng et al. [22] also studied subsonic and supersonic flows over open-cavity geometries by an unsteady NS solver based on the CESE method. When compared with experimental and analytical data, the generation and propagation of flow-induced acoustic waves were faithfully captured, and satisfactory results were obtained for the oscillation frequency of the dominant mode.

9.3 Solid Dynamics

In recent years, high-resolution discontinuity-capturing numerical methods originally devised for CFD problems have been utilized to solve nonlinear solid-dynamic problems with Eulerian formulations. Among these methods, the CESE method has attracted considerable attention from researchers in computational solid dynamics because of its simple logic, high accuracy, and ability to capture the behaviours of nonlinear waves.

Wang et al. [23] investigated numerically two high-velocity impact problems in elastic–plastic materials: (1) Taylor copper-bar-impact problem and (2) the penetration of a long rod (tungsten heavy alloy) into a steel target. In this study, the CESE method combined with the level-set technique was adopted to solve Eulerian governing equations that describe the solid dynamics and to trace material interfaces. Chen et al. [24] extended the CESE solver developed by Wang et al. [23] to simulate high-velocity impact problems involving elastic–plastic flows, high strain rates, and spall fractures. Excellent agreement was observed between their simulation of aluminium plates colliding with stainless-steel plates and the experimental data.

As known, the governing equations of elastic waves in solids can be properly written as a set of fully coupled first-order hyperbolic PDEs, including the conservation laws of mass and momentum as well as the rate-type constitutive relations for materials, by treating the density, velocity, and stress components as primitive unknowns. Therefore, the CESE method, which is suitable for hyperbolic systems, can be intuitively applied to simulate linear and nonlinear waves in elastic solids. The CESE simulations of resonant standing waves arising from a time-harmonic external axial load and compression waves arising from a bi-material collinear impact was demonstrated by Yu et al. [25]. Another study on the propagation and reflection of extensional waves in an abruptly stopped elastic rod using the CESE method was carried out by Yang et al. [26]. Moreover, Chen et al. [27] performed CESE simulations to study planar-wave expansion from a point source in an anisotropic solid of cubic symmetry (gallium arsenide) and Yang et al. [28] extended the CESE simulations to stress waves in solids of hexagonal symmetry, illustrating wave propagation in a heterogeneous solid composed of three blocks of beryl with different lattice orientations. Lately, Lowe et al. [29] conducted a comprehensive study of nonlinear longitudinal waves (including both weak and strong shocks, rarefactions, and contact discontinuities) in tapered elastic rods using the CESE method as a numerical tool. In the above studies, the CESE simulations effectively captured waves in a variety of solid materials and provided results consistent with the available analytical solutions.

9.4 Magnetohydrodynamics

The plasma flows in aerospace applications and astrophysics can be described and solved generally by the magnetohydrodynamic (MHD) equations, which combine the NS equations for fluid dynamics and the Maxwell equations for electromagnetics. Due to the divergence-free constraint usually imposed for the magnetic field \mathbf{B} in the computational MHD problems, some special treatments are added into the MHD numerical schemes to enforce $\nabla \cdot \mathbf{B} = 0$. Since the proposal of the CESE method, researchers have been attempting to solve MHD problems accurately and efficiently with the CESE method.

Zhang et al. [30, 31] used the CESE method to study MHD benchmark problems, including an MHD shock-tube problem and an MHD vortex problem. Their CESE results without additional treatments for $\nabla \cdot \mathbf{B} = 0$ compared favourably with previously reported reference solutions. In fact, Zhang et al. [30, 31] performed the simulations with the baseline CESE scheme and the CESE scheme in conjunction with a special treatment to maintain $\nabla \cdot \mathbf{B} = 0$. Nevertheless, no obvious difference was observed.

Feng et al. [32] developed a numerical platform based on the CESE method to investigate solar–interplanetary physics and space weather. Three dimensional MHD equations were solved with the adaptive mesh refinement (AMR) to better resolve flow features that have spatial scales many orders of magnitude smaller than the vast size of solar–interplanetary space. This CESE-based MHD-simulation approach was validated through the numerical study of solar corona and solar wind and comparison with observation data. Recently, Yang et al. [33, 34] extended this CESE-based MHD solver to a high-order version [33] and an upwind version [34] based on the CESE modifications of Shen et al. [35] and Shen and Wen [36], respectively. Numerical tests of MHD-vortex and MHD-blast-wave problems demonstrated the accuracy improvement of the CESE results by applying both the high-order and the upwind extension. Furthermore, a new strategy to keep the magnetic field fundamentally divergence-free was proposed by Yang et al. [33], taking the advantage of the CESE method that the spatial derivatives of the magnetic field are treated as marching variables in the algorithm.

Notably, the successful combination of MHD modelling and CESE simulation was elaborated in a recent monograph of Feng [37]. For more details about the CESE method for MHD, readers are recommended to refer to Feng [37] and the references therein.

References

1. Fedorov, A., & Tumin, A. (2004). Evolution of disturbances in entropy layer on blunted plate in supersonic flow. *AIAA Journal*, 42(1), 89–94.
2. Tseng, T., & Yang, R. J. (2005). Simulation of the Mach reflection in supersonic flows by the CE/SE method. *Shock Waves*, 14(4), 307–311.

3. Chang, I. S., Chang, C. L., & Chang, S. C. (2005). Unsteady Navier-Stokes rocket nozzle flows. In *41st AIAA/ASME/SAE/ASEE Joint Propulsion Conference and Exhibit*.
4. Chang, C. L., Venkatachari, B. S., & Cheng, G. (2006). Effect of counterflow jet on a supersonic reentry capsule. In *42nd AIAA/ASME/SAE/ASEE Joint Propulsion Conference and Exhibit*.
5. Venkatachari, B. S., Ito, Y., Cheng, G., & Chang, C. L. (2011). Numerical investigation of the interaction of counterflowing jets and supersonic capsule flows. In *42nd AIAA Thermophysics Conference*.
6. Chang, C. L., & Choudhari, M. M. (2011). Hypersonic viscous flow over large roughness elements. *Theoretical and Computational Fluid Dynamics*, 25(1), 85–104.
7. Shen, H., Wen, C. Y., & Saldívar Massimi, H. (2014). Application of CE/SE method to study hypersonic non-equilibrium flows over spheres. In *19th AIAA International Space Planes and Hypersonic Systems and Technologies Conference*.
8. Massimi, H., Shen, H., & Wen, C. Y. (2017). Study of hypersonic dissociating flows over spheres using the space-time CE/SE method. In *30th International Symposium on Shock Waves* (Vol. 1). Springer.
9. Wen, C. Y., Saldívar, H., & Shen, H. (2018). Extension of CE/SE method to non-equilibrium dissociating flows. *Journal of Computational Physics*, 356, 240–260.
10. Knab, O., Fruehauf, H. H., & Messerschmid, E. (1995). Theory and validation of the physically consistent coupled vibration-chemistry-vibration model. *Journal of Thermophysics and Heat Transfer*, 9(2), 219–226.
11. Wen, C. Y., & Hornung, H. (1995). Non-equilibrium dissociating flow over spheres. *Journal of Fluid Mechanics*, 299, 389–405.
12. Massimi, H., Shen, H., & Wen, C. Y. (2015). Numerical simulation of ionized hypersonic flows using the space-time CE/SE method. In *20th AIAA International Space Planes and Hypersonic Systems and Technologies Conference*.
13. Candler, G. V., & MacCormack, R. W. (1991). Computation of weakly ionized hypersonic flows in thermochemical nonequilibrium. *Journal of Thermophysics and Heat Transfer*, 5(3), 266–273.
14. Wang, X. Y., Chang, S. C., & Jorgenson, P. (1999). Accuracy study of the space-time CE/SE method for computational aeroacoustics problems involving shock waves. In *38th Aerospace Sciences Meeting and Exhibit*.
15. Loh, C. Y., Hultgren, L. S., & Chang, S. C. (2001). Wave computation in compressible flow using space-time conservation element and solution element method. *AIAA journal*, 39(5), 794–801.
16. Chang, S. C., Loh, C., Yu, S. T., Himansu, A., Wang, X. Y., Jorgenson, P., Chang, S. C., Loh, C., Yu, S. T., & Himansu, A. (1997). Robust and simple non-reflecting boundary conditions for the space-time conservation element and solution element method. In *13th Computational Fluid Dynamics Conference*.
17. Yen, J., Duell, E., & Martindale, W. (2006). CAA using 3D CESE method with a simplified Courant number insensitive scheme. In *12th AIAA/CEAS Aeroacoustics Conference (27th AIAA Aeroacoustics Conference)*.
18. Yen, C. C. (2011). Demonstration of a multi-dimensional time-accurate local time stepping CESE method. In *17th AIAA/CEAS Aeroacoustics Conference (32nd AIAA Aeroacoustics Conference)*.
19. Loh, C. Y., & Zaman, K. (2002). Numerical investigation of transonic resonance with a convergent-divergent nozzle. *AIAA Journal*, 40(12), 2393–2401.
20. Zaman, K., Dahl, M., Bencic, T., & Loh, C. (2002). Investigation of a ‘transonic resonance’ with convergent-divergent nozzles. *Journal of Fluid Mechanics*, 463, 313–343.
21. Kim, C. K., Yu, S. T. J., & Zhang, Z. C. (2004). Cavity flows in a scramjet engine by the space-time conservation and solution element method. *AIAA Journal*, 42(5), 912–919.
22. Cheng, G. C., Olcmen, S., Venkatachari, B. S., Brooker, B. T., & Chang, S. C. (2018). Computational study of subsonic and supersonic acoustic cavity flows using CESE method. In *2018 AIAA/CEAS Aeroacoustics Conference*.

23. Wang, J. T., Liu, K. X., & Zhang, D. L. (2009). An improved CE/SE scheme for multi-material elastic–plastic flows and its applications. *Computers & Fluids*, 38(3), 544–551.
24. Chen, Q. Y., Wang, J. T., & Liu, K. X. (2010). Improved CE/SE scheme with particle level set method for numerical simulation of spall fracture due to high-velocity impact. *Journal of Computational Physics*, 229(19), 7503–7519.
25. Yu, S. T. J., Yang, L., Lowe, R. L., & Bechtel, S. E. (2010). Numerical simulation of linear and nonlinear waves in hypoelastic solids by the CESE method. *Wave Motion*, 47(3), 168–182.
26. Yang, L., Lowe, R. L., Yu, S. T. J., & Bechtel, S. E. (2010). Numerical solution by the CESE method of a first-order hyperbolic form of the equations of dynamic nonlinear elasticity. *Journal of Vibration and Acoustics*, 132(5).
27. Chen, Y. Y., Yang, L., & Yu, S. T. J. (2011). Simulations of waves in elastic solids of cubic symmetry by the conservation element and solution element method. *Wave Motion*, 48(1), 39–61.
28. Yang, L., Chen, Y. Y., & Yu, S. T. J. (2011). Velocity-stress equations for waves in solids of hexagonal symmetry solved by the space-time CESE method. *Journal of Vibration and Acoustics*, 133(2).
29. Lowe, R. L., Lin, P. H., Yu, S. T. J., & Bechtel, S. E. (2016). An Eulerian model for nonlinear waves in elastic rods, solved numerically by the CESE method. *International Journal of Solids and Structures*, 94, 179–195.
30. Zhang, M., Yu, S. T. J., Lin, S. C., Chang, S. C., & Blankson, I. (2004). Solving magneto-hydrodynamic equations without special treatment for divergence-free magnetic field. *AIAA Journal*, 42(12), 2605–2608.
31. Zhang, M., Yu, S. T. J., Lin, S. C. H., Chang, S. C., & Blankson, I. (2006). Solving the MHD equations by the space–time conservation element and solution element method. *Journal of Computational Physics*, 214(2), 599–617.
32. Feng, X. S., Xiang, C. Q., Zhong, D. K., Zhou, Y. F., Yang, L. P., & Ma, X. P. (2014). SIP-CESE MHD model of solar wind with adaptive mesh refinement of hexahedral meshes. *Computer Physics Communications*, 185(7), 1965–1980.
33. Yang, Y., Feng, X. S., & Jiang, C. W. (2017). A high-order CESE scheme with a new divergence-free method for MHD numerical simulation. *Journal of Computational Physics*, 349, 561–581.
34. Yang, Y., Feng, X. S., & Jiang, C. W. (2018). An upwind CESE scheme for 2D and 3D MHD numerical simulation in general curvilinear coordinates. *Journal of Computational Physics*, 371, 850–869.
35. Shen, H., Wen, C. Y., Liu, K. X., & Zhang, D. L. (2015). Robust high-order space–time conservative schemes for solving conservation laws on hybrid meshes. *Journal of Computational Physics*, 281, 375–402.
36. Shen, H., & Wen, C. Y. (2016). A characteristic space–time conservation element and solution element method for conservation laws II. Multidimensional extension. *Journal of Computational Physics*, 305, 775–792.
37. Feng, X. S. (2019). *Magnetohydrodynamic modeling of the solar corona and heliosphere*. Springer.

Open Access This chapter is licensed under the terms of the Creative Commons Attribution 4.0 International License (<http://creativecommons.org/licenses/by/4.0/>), which permits use, sharing, adaptation, distribution and reproduction in any medium or format, as long as you give appropriate credit to the original author(s) and the source, provide a link to the Creative Commons license and indicate if changes were made.

The images or other third party material in this chapter are included in the chapter's Creative Commons license, unless indicated otherwise in a credit line to the material. If material is not included in the chapter's Creative Commons license and your intended use is not permitted by statutory regulation or exceeds the permitted use, you will need to obtain permission directly from the copyright holder.

